Infrared Physics & Technology 75 (2016) 133–138

Contents lists available at ScienceDirect

Infrared Physics & Technology

journal homepage: www.elsevier.com/locate/infrared

# Investigation on low thermal emittance of Al films deposited by magnetron sputtering

Yuping Ning [a], Wenwen Wang [a], Ying Sun [a], Yongxin Wu [a], Yingfang Liu [a], Hongliang Man [a], Cong Wang [a,b,*], Yong Zhang [c], Shuxi Zhao [d], Eric Tomasella [e], Angélique Bousquet [e]

[a] Center for Condensed Matter and Material Physics, Department of Physics, Beihang University, Beijing 100191, China
[b] Pneumatic and Thermodynamic Energy Storage and Supply Beijing Key Laboratory, Beijing, China
[c] State Key Laboratory for Advanced Metals and Materials, University of Science and Technology Beijing, Beijing 100083, China
[d] Ångström Laboratory, Uppsala University, P.O. Box 534, SE-751 21 Uppsala, Sweden
[e] Clermont Université, Université Blaise Pascal, Institute of Chemistry of Clermont-Ferrand (ICCF), CNRS-UMR 6296, 24 Avenue des Landais, 63171 Aubière, France

## HIGHLIGHTS

- Optimal thickness 78 nm of Al film for lowest emittance is obtained.
- Emittance of optimal Al film keeps close to 0.02 from 25 °C to 400 °C.
- Optical constants of Al film are deduced by fitting R and T spectra.

## ARTICLE INFO

*Article history:*
Received 17 October 2015
Available online 23 January 2016

*Keywords:*
Al film
Thermal emittance
Film thickness
Optical constant

## ABSTRACT

A series of Al films with different thicknesses were deposited on polished stainless steel by direct current (DC) magnetron sputtering as a metal IR-reflector layer in solar selective absorbing coating (SSAC). The effects of the film thickness and the temperature on the thermal emittance of the Al films are studied. An optimal thickness 78 nm of the Al film for the lowest total thermal emittance is obtained. The thermal emittance of the optimal Al film keeps close to 0.02 from 25 °C to 400 °C, which are low enough to satisfy the optical requirements in SSAC. The optical constants of the Al film are deduced by fitting the reflectance and transmission spectra using SCOUT software.



## 1. Introduction

Solar selective absorbing coatings (SSACs) which are one of the key elements of the solar collectors are used as the photothermal conversion surface [1–4]. An ideal SSAC should both have a high absorptance (near one) in the solar spectrum range (0.3–2.5 μm), and a low thermal emittance (near zero) in the thermal infrared range (>2.5 μm) as shown in Fig. 1 [5,6]. The typical double cermet layer structure of SSAC from surface to substrate is showed in Fig. 2, which is composed of the following: (i) an antireflection (AR) layer that enhances solar transmission; (ii) a low metal volume fraction (LMVF) cermet solar absorption layer, a high metal volume fraction (HMVF) cermet solar absorption layer, which forms interference absorption bilayer; (iii) a metal IR-reflector layer that reduces the thermal emittance from the substrate; (iv) a substrate [7,8].

The optical properties of the SSAC are characterized by two important parameters: solar absorptance ($\alpha$) and thermal emittance ($\varepsilon$). Generally, $\alpha \geqslant 0.95$ and $\varepsilon \leqslant 0.05$ at room temperature are necessary for the requirement of optical property of a SSAC. The stainless steel (SS) is always used as the substrate in the industry production for its low costs and high temperature stability. But the thermal emittance of the SS is high, such as $\varepsilon(25\ ^\circ C) = 0.10$ for a 304SS with a polished surface. A metal IR-reflector layer with a low emittance must be deposited on the SS substrate in order to reduce the thermal emittance of the SS substrate. When the upper three layers (HMVF, LMVF and AR) are deposited sequentially on the metal IR-reflector, the chemical structure of the metal IR-reflector keeps stability and the interface forms between the metal IR-reflector and the upper HMVF layer [9–12]. Thus the thermal emittance of the metal IR-reflector maintains. And the thermal emittance increment after depositing the upper three layers can

* Corresponding author at: Center for Condensed Matter and Material Physics, Department of Physics, Beihang University, Beijing 100191, China.

http://dx.doi.org/10.1016/j.infrared.2016.01.007
1350-4495/

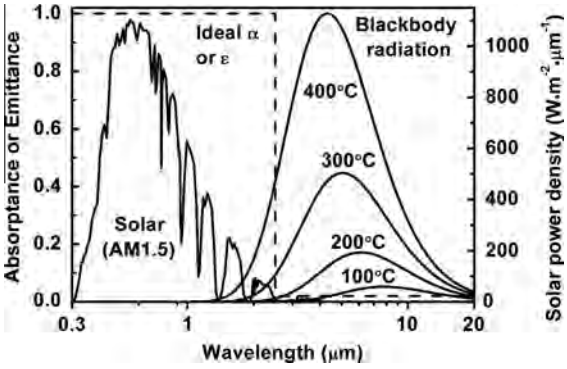


**Fig. 1.** The absorptance or emittance spectrum of an ideal solar selective absorbing coating (SSAC).

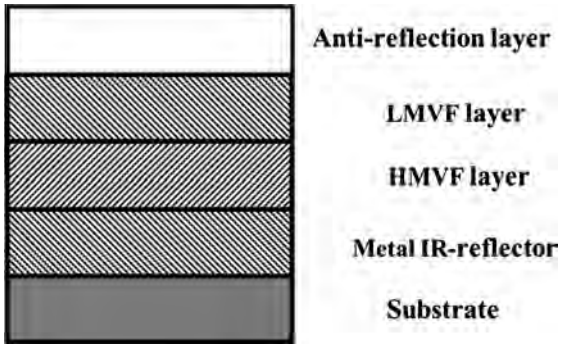


**Fig. 2.** Schematic diagram of the typical double cermet layer structure for solar selective absorbing coating (SSAC).

be minimized by tuning the extinction coefficient to zero in the thermal infrared range or reducing the film thicknesses of the upper three layers [13,14]. The metal IR-reflector layer with low emittance is essential to obtain a low emittance for SSAC [11,15]. Therefore, it is important to choose appropriately and prepare successfully a metal layer with low emittance for SSAC.

According to Hagen–Rubens relation [16] for the long wavelength radiation, the normal reflectance of the metal is obtained from Eq. (1):

$$\rho_n^s = 1 - 0.365\sqrt{\gamma/\lambda} \tag{1}$$

$\lambda$ is wavelength (cm) and $\gamma$ is electrical resistivity (Ω·cm). Therefore the smaller the electrical resistivity is, the higher the normal reflectance of the metal, which is the theoretical foundation to choose metal with high IR reflectance. The reasons for selecting the metal Al as the metal IR-reflector are as follows. The metal Al with very low electrical resistivity will ensure high IR reflectance, i.e. low thermal emittance. SSACs with Al metal IR-reflector have low thermal emittance, such as Al/M-AlN/AlN: $\varepsilon$ (25 °C) = 0.03–0.04, $\varepsilon$(350 °C) = 0.07–0.10 [17]; Al/W-AlON/AlON: $\varepsilon$(80 °C) = 0.051 [13]; Al/Zr–$ZrO_2$/$Al_2O_3$: $\varepsilon$(80 °C) = 0.049 [18]; Al/$Ti_xAl_yN$/AlN: $\varepsilon$(82 °C) = 0.04–0.06 [10]; Al/NbMoN/NbMoON/$SiO_2$: $\varepsilon$(80 °C) = 0.05 [19]. Additionally, the metal Al is cheaper and the SSACs using the metal Al as the IR-reflector have good thermal stability up to 400 °C both in vacuum and air [10,19]. But the detailed information about the relationship between the emittance of the Al films and the film thickness, temperature, etc. has not been reported so far. Considering the widely usage of the Al films in SSACs, it is valuable to study the thermal emittance and relevant optical properties of the Al films.

According to our research, the substrate surface condition has a great influence on the thermal emittance of the metal films on it and the smooth substrate surface can ensure a low emittance of the metal films. Thus, the 304SS with mirror polished surface, of roughness average (*Sa*) 1.01 nm is used as the substrate to eliminate the effect of substrate surface conditions.

In this paper, the Al films were prepared on 304SS substrate with mirror polished surface by DC magnetron sputtering as the IR-reflector metal layer in SSAC. The effect of the film thickness on the thermal emittance is studied and the optimal thickness which makes the thermal emittance the lowest is obtained. The effect and reason of the temperature on the thermal emittance are discussed. Moreover, the structure, morphologies and optical constants of the Al films are investigated in detail.

## 2. Experiments

The Al films were deposited by a JGP350C magnetron sputtering equipment. The size of Al target is Φ60 mm × 3 mm. The substrates were chemically cleaned in an ultrasonic agitator using alcohol followed by de-ionized water rising and air drying before being deposited. The detailed preparation parameters are in Table 1.

The crystal structure of the Al film was characterized by X-ray diffraction (XRD) on a Dmax diffractometer with Cu Kα radiation. The surface morphologies of the Al film and substrate surface roughness were observed by scanning electron microscopy (SEM) FEI XLS30 and atomic force microscopy (AFM) CSPM400. The film thickness was measured using a Dektak 6 M surface profiler.

Normal reflectance data were measured by spectrometer L900 (0.3–2.5 μm) and Fourier Transform Infrared Reflectance (FTIR) spectrometer Bruker Tensor 27 (2.5–22 μm). The reflectance data in the range of 23–100 μm are extrapolated. Both instruments are equipped with integrated spheres to reduce scattering effect. The total thermal emittance with a normal angle of radiation is calculated according to Eq. (2) which is weighted by the blackbody radiation, for the given temperature $T$ [20], where $\lambda_1$ depends on temperature and $\lambda_2$ = 100 μm.

$$\varepsilon_T = \frac{\int_{\lambda_1}^{\lambda_2}(1 - R(\lambda))I_b(\lambda, T)d\lambda}{\int_{\lambda_1}^{\lambda_2} I_b(\lambda, T)d\lambda} \tag{2}$$

## 3. Results and discussion

### 3.1. Structure and morphologies of the Al film

The measured XRD pattern of the Al film is showed in Fig. 3. The Al film with cubic structure (PDF: 04-0787) grows preferentially along the (1 1 1) direction. The smooth and dense surface of the Al film with the thickness of 78 nm on SS substrate is showed in Fig. 4. The surface average roughness (*Sa*) of the SS substrate is 1.01 nm and increased to 4.08 nm when the Al film with the thickness of 78 nm was deposited on the SS substrate (see Fig. 5).

**Table 1**
Parameters for the deposition of the Al films.

| Sputtering method | DC |
|---|---|
| Base vacuum | $1 \times 10^{-3}$ (Pa) |
| Substrate-to-target distance | 60 (mm) |
| Ar gas flow rate | 50 (sccm) |
| Sputtering pressure | 0.3 (Pa) |
| Target power density | 7.2 (W/cm$^2$) |

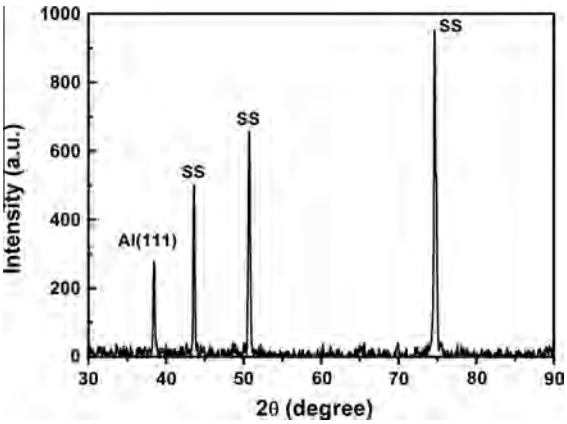


**Fig. 3.** XRD pattern of the Al film on SS substrate.

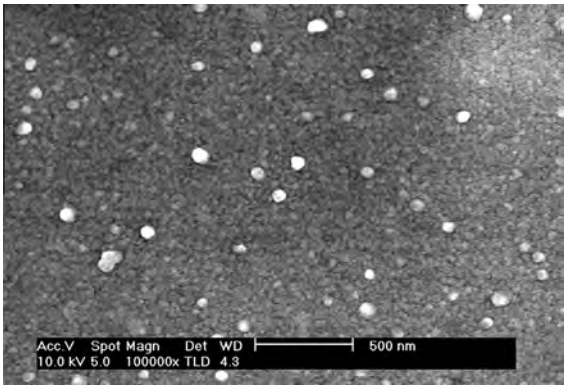


**Fig. 4.** SEM morphology of the Al film with the thickness of 78 nm on SS substrate.

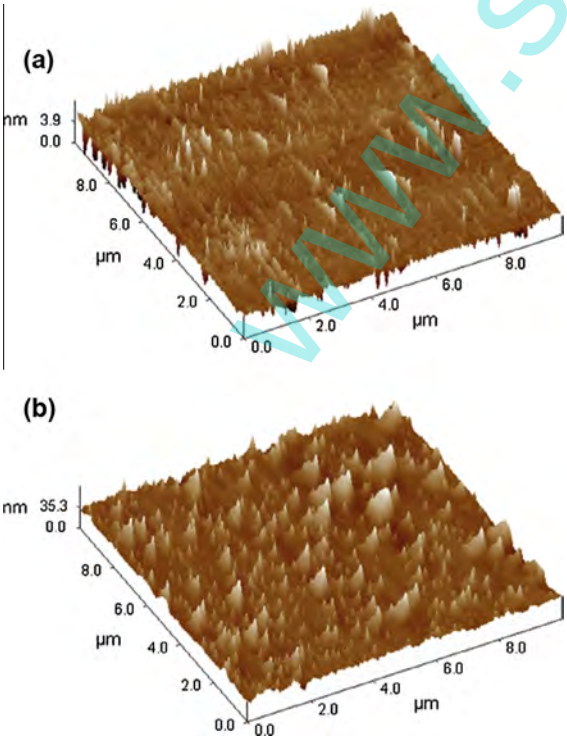


**Fig. 5.** AFM morphology of (a) the SS substrate with mirror polished surface; (b) Al film with the thickness of 78 nm on this SS substrate.

### 3.2. Thermal emittance of the Al films

#### 3.2.1. Effect of film thickness on thermal emittance

Fig. 6(a) shows the reflectance spectra of the Al films with increasing thickness: 4 nm, 12 nm, 19 nm, 39 nm, 78 nm, 117 nm, 194 nm. Fig. 6(b) is the partial enlarged image of Fig. 6(a) which reveals the slight change of the reflectance spectra with increasing thickness. The reflectance increases gradually from 4 nm to 19 nm, and then reaches the maximum in the thickness range of 39 nm to 117 nm, and decreases when the thickness reaches 194 nm.

The variations of the reflectance spectra of the Al film attributes to its film growing process. The Al film consists of tiny crystals with hill-like rounded top initially and then grows to a dense smooth surface because of the broadening of the hill-like tops with increasing film thickness (from 4 nm to 19 nm). The dense and smooth surface of the Al film keeps unchanged with the continually increasing thickness from 39 nm to 117 nm, of which the reflectance spectra are nearly the same and reach the maximum. The columnar holes and rough surface form with the continually increasing film thickness (increasing to 194 nm), due to the shielding of the columnar grains, forming deep grooves among the hill-like tops, new interlaced hill-like tops and columnar grains. These microstructures absorb light which makes the reflectance decrease. The thickness range for the highest reflectance of the Al film is from 39 nm to 117 nm.

Fig. 7 shows the thermal emittance of the Al films with different temperatures from 25 °C to 400 °C as the film thickness increases. The thermal emittance decreases rapidly with film thickness less than 50 nm, and reaches the minimum value approaching 0.02 at 78 nm, and then increases slightly with increasing film thickness continually. Hence, the optimal thickness of the Al film which

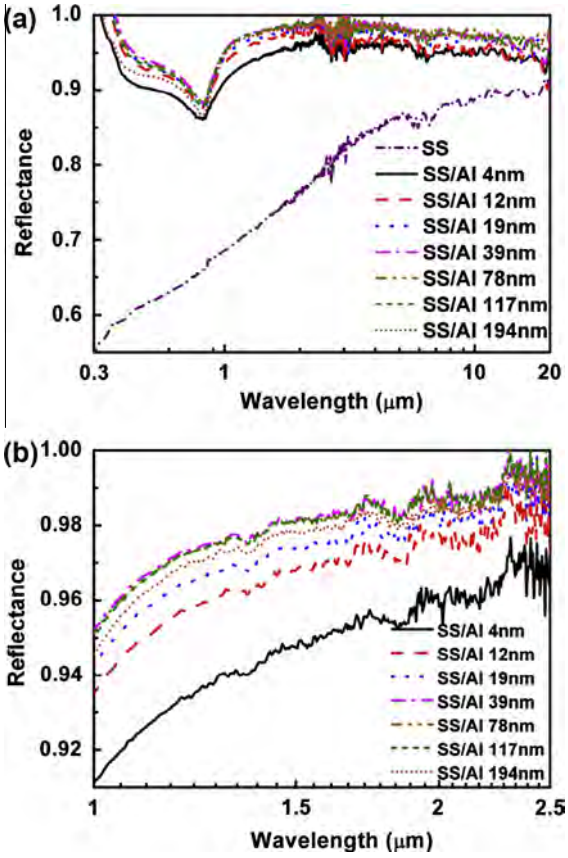


**Fig. 6.** Reflectance spectra of the Al films with different thicknesses (a) the whole spectra from 0.3 μm to 20 μm; (b) the partial enlarged spectra from 1 μm to 2.5 μm.

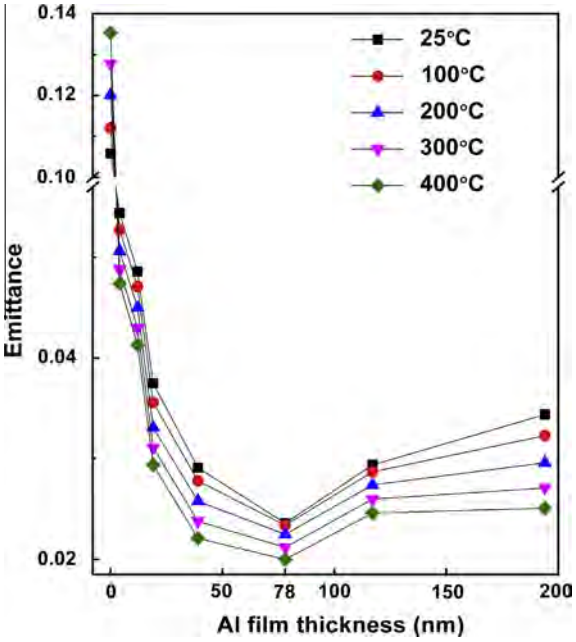


**Fig. 7.** The thermal emittance of the Al films at different temperatures as a function of the film thickness.

makes the thermal emittance the lowest is 78 nm. The thermal emittance of the Al films decreases with increasing temperature, which will be discussed in detail in next section.

### 3.2.2. Effect of temperature on thermal emittance

Fig. 8 shows the changing trends of the thermal emittance of the Al film with the increasing of the temperature. The thermal emittance of samples SS/Al films decreases gradually with increasing temperature, whereas the thermal emittance for the SS substrate increases. The changing of reflectance spectra of them results in these phenomena, which will be explained below.

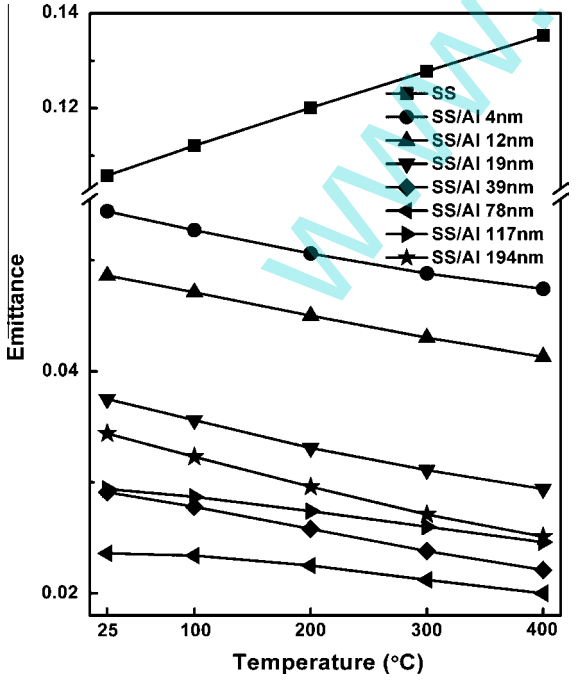


**Fig. 8.** The thermal emittance of the Al films with different thicknesses as a function of the temperature.

The thermal emittance of Al film is the lowest at the optimal thickness of 78 nm, which are $\varepsilon(25\ ^\circ C) = 0.024$, $\varepsilon(100\ ^\circ C) = 0.023$, $\varepsilon(200\ ^\circ C) = 0.023$, $\varepsilon(300\ ^\circ C) = 0.021$, $\varepsilon(400\ ^\circ C) = 0.020$, respectively. All the thermal emittance values approach to 0.02, which satisfy the property requirement for the metal IR-reflector in SSACs.

According to Eq. (2), makes

$$\int_{\lambda_1}^{\lambda_2} I_b(\lambda, T)d\lambda = A(T) \tag{3}$$

Eq. (4) is obtained via substituting Eq. (3) into Eq. (2):

$$\varepsilon_T = \int_{\lambda_1}^{\lambda_2} (1 - R(\lambda))\frac{I_b(\lambda, T)}{A(T)}d\lambda = \int_{\lambda_1}^{\lambda_2} (1 - R(\lambda))I'_b(\lambda, T)d\lambda \tag{4}$$

According to Eq. (4), the thermal emittance is the function of $R(\lambda)$ and $\acute{I}_b(\lambda, T)$, where $\acute{I}_b(\lambda, T)$ is only determined by temperature. Thus, the thermal emittance at the given temperature is only determined by the reflectance spectra of the samples. Therefore, the changing trends of the thermal emittance are resulted from the variation of the reflectance spectra.

The reflectance $R(\lambda)$, $(1 - R(\lambda))$ and $\acute{I}_b(\lambda, T)$ of the SS substrate and sample SS/Al (78 nm) are shown in Fig. 9. For the sample SS/Al (78 nm), the reflectance $R(\lambda)$ decreases and $(1 - R(\lambda))$ increases monotonically as the wavelength increasing. The intensity of the $\acute{I}_b(\lambda, T)$ rises with increasing temperature and the corresponding wavelength of the maximum intensity moves to the short wavelength. Thus, the thermal emittance of the SS/Al (78 nm) decreases as the temperature increasing according to Eq. (4), whereas the case is opposite for the SS substrate.

### 3.3. Optical constants of the Al film

Fig. 10 shows the measured and theoretically fitted reflectance and transmittance spectra of the Al film with thickness of 12 nm. The simulation is done by SCOUT software [21]. The dielectric function model of the Al film consists of three parts [22]: The Drude model (the free electron contribution) which describes the intraband contributions to the optical properties; The OJL model suggested by O'Leary [23] based on the joint density of states describes the interband transition contribution. This function models the strong interband transition at the wavelength around 0.8 μm; The Kim oscillators suggested by Kim [24] model the weak broad interband absorption in the wavelength range from 0.3 μm to 2.5 μm.

The deduced optical constants of the sputtering film Al and the bulk Al in reference [25] are shown in Fig. 11. Both values of refractive index ($n$) and extinction coefficient ($k$) of the film Al are higher

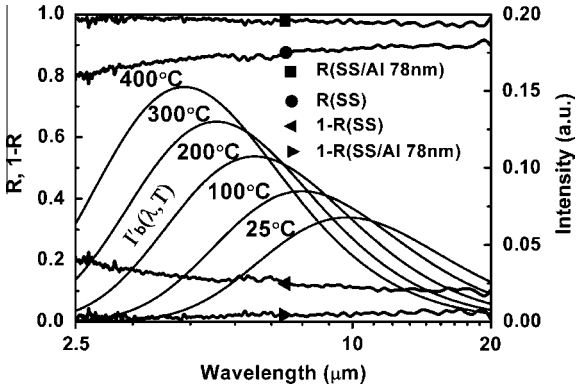


**Fig. 9.** The $R(\lambda)$, $(1 - R(\lambda))$ and $\acute{I}_b(\lambda, T)$ of the SS substrate and SS/Al (78 nm).

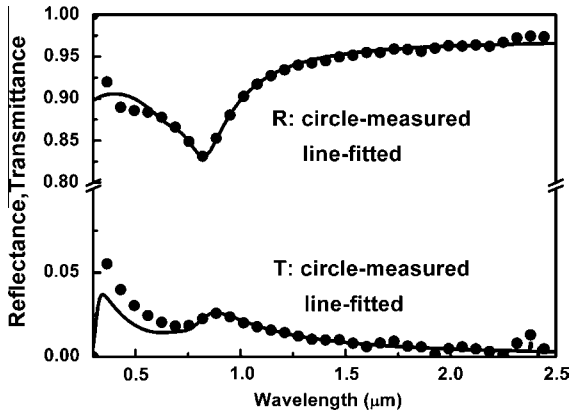


**Fig. 10.** Measured and fitted reflectance and transmittance spectra of the Al film with thickness of 12 nm, deposited on microslide glass substrate.

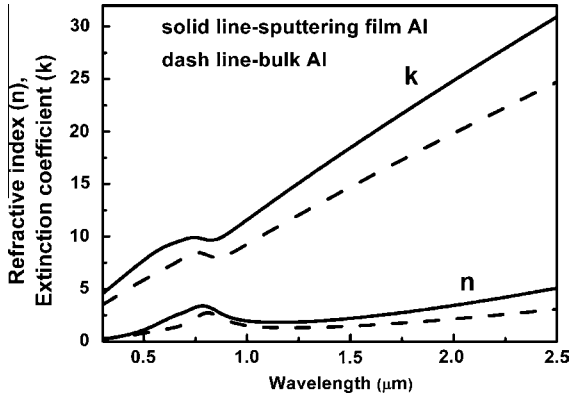


**Fig. 11.** Optical constants of the experimental sputtering film Al compared with that of the bulk Al.

than bulk Al's. The varying trends of n, k of the film Al and the bulk Al are accordant.

The simulated reflectance spectra of the Al films with the thickness of 12 nm, 19 nm and 78 nm, respectively, are shown in Fig. 12, based on the deduced optical constants. They are in good agreement with the measured ones which means that the deduced optical constants of the Al film are accurate enough and can be used for the simulation of the SSAC including a metal Al IR-reflector further.

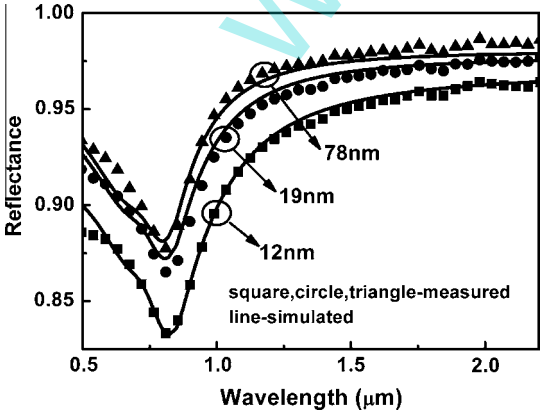


**Fig. 12.** Measured and simulated reflectance spectra of the Al films with thickness of 12 nm, 19 nm and 78 nm, respectively, deposited on the microslide glass substrate.

## 4. Conclusions

The Al films with cubic lattice are prepared, which grow preferentially along the (1 1 1) direction. The optimal thickness 78 nm of the Al film for the lowest thermal emittance is obtained, and the thermal emittance values of the optimal Al film at the temperature from 25 °C to 400 °C are close to 0.02. The optimal Al film is qualified as the metal IR-reflector in SSACs. The optical constants of the Al film are deduced by fitting the reflectance and transmittance spectra, which can be used for the optical simulation of the SSACs.

## Conflict of interest

There is no conflict of interest.

## Acknowledgements

The authors acknowledge the financial support by Aeronautical Science Foundation of China (2014ZF51067), State Key Lab of Advanced Metals and Materials (2014-ZD03) and the Beijing Key Subject Foundation of Condensed Matter Physics.

## References

[1] L. Rebouta, P. Capela, M. Andritschky, A. Matilainen, P. Santilli, K. Pischow, E. Alves, Characterization of TiAlSiN/TiAlSiON/$SiO_2$ optical stack designed by modelling calculations for solar selective applications, Sol. Energy Mater. Sol. Cells 105 (2012) 202–207.
[2] N. Selvakumar, S. Santhoshkumar, S. Basu, A. Biswas, H.C. Barshilia, Spectrally selective CrMoN/CrON tandem absorber for mid-temperature solar thermal applications, Sol. Energy Mater. Sol. Cells 109 (2013) 97–103.
[3] J.X. Feng, S. Zhang, Y. Lu, H.W. Yu, L.M. Kang, X.Y. Wang, Z.M. Liu, H.C. Ding, Y. Tian, J. Ouyang, The spectral selective absorbing characteristics and thermal stability of SS/TiAlN/TiAlSiN/$Si_3N_4$ tandem absorber prepared by magnetron sputtering, Sol. Energy 111 (2015) 350–356.
[4] J. Wang, B.C. Wei, Q.R. Wei, D.J. Li, Optical property and thermal stability of Mo/Mo–$SiO_2$/$SiO_2$ solar-selective coating prepared by magnetron sputtering, Phys. Status Solidi A 208 (2011) 664–667.
[5] Y.F. Xue, C. Wang, Y. Sun, Y.X. Wu, Y.P. Ning, W.W. Wang, Effects of the LMVF and HMVF absorption layer thickness and metal volume fraction on optical properties of the $MoSi_2$–$Al_2O_3$ solar selective absorbing coating, Vacuum 104 (2014) 116–121.
[6] C.E. Kennedy, Review of mid- to high temperature solar selective absorber materials, Technical Report, 2002.
[7] Q.C. Zhang, D.R. Mills, New cermet film structures with much improved selectivity for solar thermal applications, Appl. Phys. Lett. 60 (1992) 545–547.
[8] Y.F. Xue, C. Wang, W.W. Wang, Y. Liu, Y.X. Wu, Y.P. Ning, Y. Sun, Spectral properties and thermal stability of solar selective absorbing AlNi–$Al_2O_3$ cermet coating, Sol. Energy 96 (2013) 113–118.
[9] L. Hao, M. Du, X.P. Liu, S.M. Wang, L.J. Jiang, F. LÜ, Z.N. Li, J. Mi, Thermal stability of nitride solar selective absorbing coatings used in high temperature parabolic trough current, Sci. China Technol. Sci. 53 (6) (2010) 1507–1512.
[10] M. Du, X.P. Liu, L. Hao, X.J. Wang, J. Mi, L.J. Jiang, Q.H. Yu, Microstructure and thermal stability of Al/$Ti_{0.5}Al_{0.5}N$/$Ti_{0.25}Al_{0.75}N$/AlN solar selective coating, Sol. Energy Mater. Sol. Cells 111 (2013) 49–56.
[11] L.Q. Zheng, F.Y. Zhou, X.G. Diao, Properties of infrared high reflectance Mo film for solar selective coatings by MF sputtering, Mater. Sci. Forum 743–744 (2013) 857–862.
[12] L.Q. Zheng, F.Y. Zhou, Z.D. Zhou, X.W. Song, G.B. Dong, M. Wang, X.G. Diao, Angular solar absorptance and thermal stability of Mo–$SiO_2$ double cermet solar selective absorber coating, Sol. Energy 115 (2015) 341–346.
[13] Q.C. Zhang, Y.G. Shen, High performance W-AlN cermet solar coatings designed by modelling calculations and deposited by DC magnetron sputtering, Sol. Energy Mater. Sol. Cells 81 (2004) 25–37.
[14] S.X. Zhao, E. Wäckelgård, Optimization of solar absorbing three-layer coatings, Sol. Energy Mater. Sol. Cells 90 (2006) 243–261.
[15] Q.C. Zhang, High efficiency Al–N cermet solar coatings with double cermet layer film structures, J. Phys. D Appl. Phys. 32 (1999) 1938–1944.
[16] M.F. Modest, Radiative Heat Transfer, second ed., Academic Press, San Diego, 2003.
[17] Q.C. Zhang, Metal–AlN cermet solar selective coatings deposited by direct current magnetron sputtering technology, J. Phys. D Appl. Phys. 31 (1998) 355–362.
[18] Q.C. Zhang, M.S. Hadavi, K.-D. Lee, Y.G. Shen, Zr–$ZrO_2$ cermet solar coatings designed by modelling calculations and deposited by dc magnetron sputtering, J. Phys. D Appl. Phys. 36 (2003) 723–729.
[19] Y.X. Wu, C. Wang, Y. Sun, Y.F. Xue, Y.P. Ning, W.W. Wang, S.X. Zhao, E. Tomasella, A. Bousquet, Optical simulation and experimental optimization of

Al/NbMoN/NbMoON/$SiO_2$ solar selective absorbing coatings, Sol. Energy Mater. Sol. Cells 134 (2015) 373–380.
[20] European Standard, EN 673, Thermal insulation of glazing calculation rules for determining the steady "U" value (thermal transmittance) of glazing, 1998.
[21] W. Theiss, in: M. Theiss (Ed.), SCOUT Thin Film Analysis Software Handbook, Hard-and Software, Aachen, Germany <http://www.mtheiss.com>.
[22] S.X. Zhao, E. Wäckelgård, The optical properties of sputtered composite of Al–AlN, Sol. Energy Mater. Sol. Cells 90 (2006) 1861–1874.
[23] S.K. O'Leary, S.R. Johnson, P.K. Lim, The relationship between the distribution of electronic states and the optical absorption spectrum of an amorphous semiconductor: an empirical analysis, J. Appl. Phys. 82 (1997) 3334.
[24] C.C. Kim, J.W. Garland, H. Abad, P.M. Raccah, Modeling the optical dielectric function of semiconductors: extension of the critical-point parabolic-band approximation, Phys. Rev. B 45 (1992) 11749.
[25] A.D. Rakić, A.B. Djurišić, J.M. Elazar, M.L. Majewski, Optical properties of metallic films for vertical-cavity optoelectronic devices, Appl. Opt. 37 (22) (1998) 5271–5283.